T-Wave Morphology Restitution Predicts Sudden Cardiac Death in Patients With Chronic Heart Failure

Julia Ramírez, PhD; Michele Orini, PhD; Ana Mincholé, PhD; Violeta Monasterio, PhD; Iwona Cygankiewicz, MD, PhD; Antonio Bayés de Luna, MD, PhD; Juan Pablo Martínez, PhD; Esther Pueyo, PhD; Pablo Laguna, PhD

Background—Patients with chronic heart failure are at high risk of sudden cardiac death (SCD). Increased dispersion of repolarization restitution has been associated with SCD, and we hypothesize that this should be reflected in the morphology of the T-wave and its variations with heart rate. The aim of this study is to propose an electrocardiogram (ECG)-based index characterizing T-wave morphology restitution (TMR), and to assess its association with SCD risk in a population of chronic heart failure patients.

Methods and Results—Holter ECGs from 651 ambulatory patients with chronic heart failure from the MUSIC (MUerte Súbita en Insuficiencia Cardiaca) study were available for the analysis. TMR was quantified by measuring the morphological variation of the T-wave per RR increment using time-warping metrics, and its predictive power was compared to that of clinical variables such as the left ventricular ejection fraction and other ECG-derived indices, such as T-wave alternans and heart rate variability. TMR was significantly higher in SCD victims than in the rest of patients (median 0.046 versus 0.039, $P<0.001$). When TMR was dichotomized at TMR=0.040, the SCD rate was significantly higher in the TMR≥0.040 group ($P<0.001$). Cox analysis revealed that TMR≥0.040 was strongly associated with SCD, with a hazard ratio of 3.27 ($P<0.001$), independently of clinical and ECG-derived variables. No association was found between TMR and pump failure death.

Conclusions—This study shows that TMR is specifically associated with SCD in a population of chronic heart failure patients, and it is a better predictor than clinical and ECG-derived variables. (***J Am Heart Assoc***. 2017;6:e005310. DOI: 10.1161/JAHA.116.005310.)

Key Words: chronic heart failure • dispersion of repolarization • repolarization restitution • sudden cardiac death • T-wave morphology

P atients with mild-to-moderate heart failure (New York Heart Association [NYHA] classes II and III) represent a high-risk population for sudden cardiac death (SCD).[1] Although implantable cardioverter defibrillators reduce SCD

mortality,[2] their cost-effectiveness is limited, with a relatively small number of patients receiving appropriate implantable cardioverter defibrillator shocks during follow-up.[2] Therefore, finding effective techniques for risk stratification able to specifically target functional or arrhythmic treatment is still a relevant unmet need with important clinical and economic implications.

The restitution of ventricular repolarization reflects the adaptation of repolarization to changes in heart rate, with the slope of the repolarization restitution indicating the variation of the action potential duration (APD) per RR increment.[3] Heterogeneity in the restitution properties across the ventricle has been reported to contribute to the establishment of repolarization dispersion gradients,[4–6] which, when accentuated, are associated with greater propensity to suffer from malignant ventricular arrhythmia.[7,8] Evaluation of the dispersion in repolarization restitution is commonly performed from invasive procedures,[9] which limit its use for risk assessment.

T-wave-derived indices have been proposed in the literature as markers of repolarization dispersion, such as the

<div style="border:2px solid red;">

Clinical Perspective

What Is New?

- The T-wave morphology restitution index (TMR) is a novel electrocardiogram marker that measures morphological changes in the T-wave as a response to heart rate variations.
- TMR specifically predicted sudden cardiac death in a population of 651 chronic heart failure patients from the MUSIC (MUerte Súbita en Insuficiencia Cardiaca) study, with no association with pump failure death.
- TMR was the strongest predictor of sudden cardiac death compared with other markers such as left ventricular ejection fraction, QRS duration, or T-wave alternans.

What Are the Clinical Implications?

- Our results support the hypothesis that increased spatio-temporal inhomogeneity in the repolarization process is arrhythmogenic.
- TMR can be automatically derived from Holter recordings and may improve sudden cardiac death risk prediction in chronic heart failure patients.

</div>

T-peak-to-end (Tpe) interval.[10] In addition, its response to changes in heart rate, here denoted by $\Delta\alpha^{Tpe}$, has been introduced as a marker of restitution dispersion.[11] An analogous analysis can be done using the QT interval, traditionally used in the clinical practice,[12] thus obtaining $\Delta\alpha^{QT}$.[13] However, these interval-based indices neglect important information regarding spatio-temporal dispersion of repolarization present in the morphology of the T-wave.[14-16] In this study we hypothesized that the variations in the morphology of the T-wave in response to variations in the RR interval (RRI) could be used as a marker of spatial heterogeneity of restitution and are associated with increased vulnerability to ventricular arrhythmias.

We applied a recently developed methodology that quantifies the morphological differences between T-waves[17] to quantify T-wave morphological change per RR increment. We called this index T-wave morphology restitution (TMR), and we demonstrated its usefulness in the prediction of arrhythmic risk leading to SCD in chronic heart failure (CHF) patients.

Methods

Study Population, Follow-Up, and End Points

The original study population consisted of 992 consecutive patients with symptomatic CHF corresponding to NYHA classes II and III enrolled in the MUSIC (MUerte Súbita en Insuficiencia Cardiaca) study, a prospective, multicenter study designed to assess risk predictors for cardiovascular mortality in ambulatory CHF patients.[18] Patients were enrolled from the specialized CHF clinics of 8 university hospitals between April 2003 and December 2004. A 2- (3%) or 3-lead (97%) 24-hour Holter ECG sampled at 200 Hz was recorded in each patient at enrollment using ELA Medical equipment (Sorin Group, Paris, France). The original cohort included patients in atrial fibrillation, in sinus rhythm, in flutter, and in pacemaker rhythm. In this work, only data from 651 patients in sinus rhythm were analyzed. The MUSIC study included patients with both reduced and preserved left ventricular ejection fraction (LVEF). Patients with preserved LVEF were included if they had CHF symptoms, a prior hospitalization for CHF or objective CHF signs confirmed by chest x-ray and/or echocardiography. Patients were excluded if they had recent acute coronary syndrome or severe valvular disease amenable for surgical repair. Patients with other concomitant diseases expected to reduce life expectancy were also excluded. The study protocol was approved by the institutional investigation committees, and all patients signed informed consent.[18]

Follow-up visits were conducted on an outpatient basis every 6 months, for a median of 44 months, until June 2007. The primary end point of this study was SCD, and the secondary end points were cardiac death (CD) and pump failure death (PFD). CD was defined as SCD if it was (1) a witnessed death occurring within 60 minutes of the onset of new symptoms, unless a cause other than cardiac was obvious; (2) an unwitnessed death (<24 hours) in the absence of preexisting progressive circulatory failure or other causes of death; or (3) a death during attempted resuscitation. Deaths occurring in hospitals as a result of refractory progressive end-stage CHF were defined as PFD. End points were reviewed and classified by the MUSIC Study Endpoint Committee.[18]

Quantification of the T-Wave Morphology Restitution

Preprocessing included low-pass filtering at 40 Hz to remove electric and muscle noise but allow QRS and T-wave analysis. Baseline wander was canceled by high-pass filtering at 0.5 Hz. Lead-wise principal component analysis was applied to choose the ECG projection that better emphasized the T-wave energy.[19] A fully automatic delineation system[20] with a posterior visual inspection to remove any possible error was used to calculate QRS and T-wave delineation marks. The computation was performed in a fully automatic manner with custom-developed software implemented at the High Performance computing platform of the NANBIOSIS ICTS, CIBER-BBN, and I3A, Zaragoza, Spain.

The hypothesis underlying the methodology presented in this work is represented in Figure 1A. The different curves represent the so-called APD restitution curves, ie, the relationship between different ventricular APDs and the
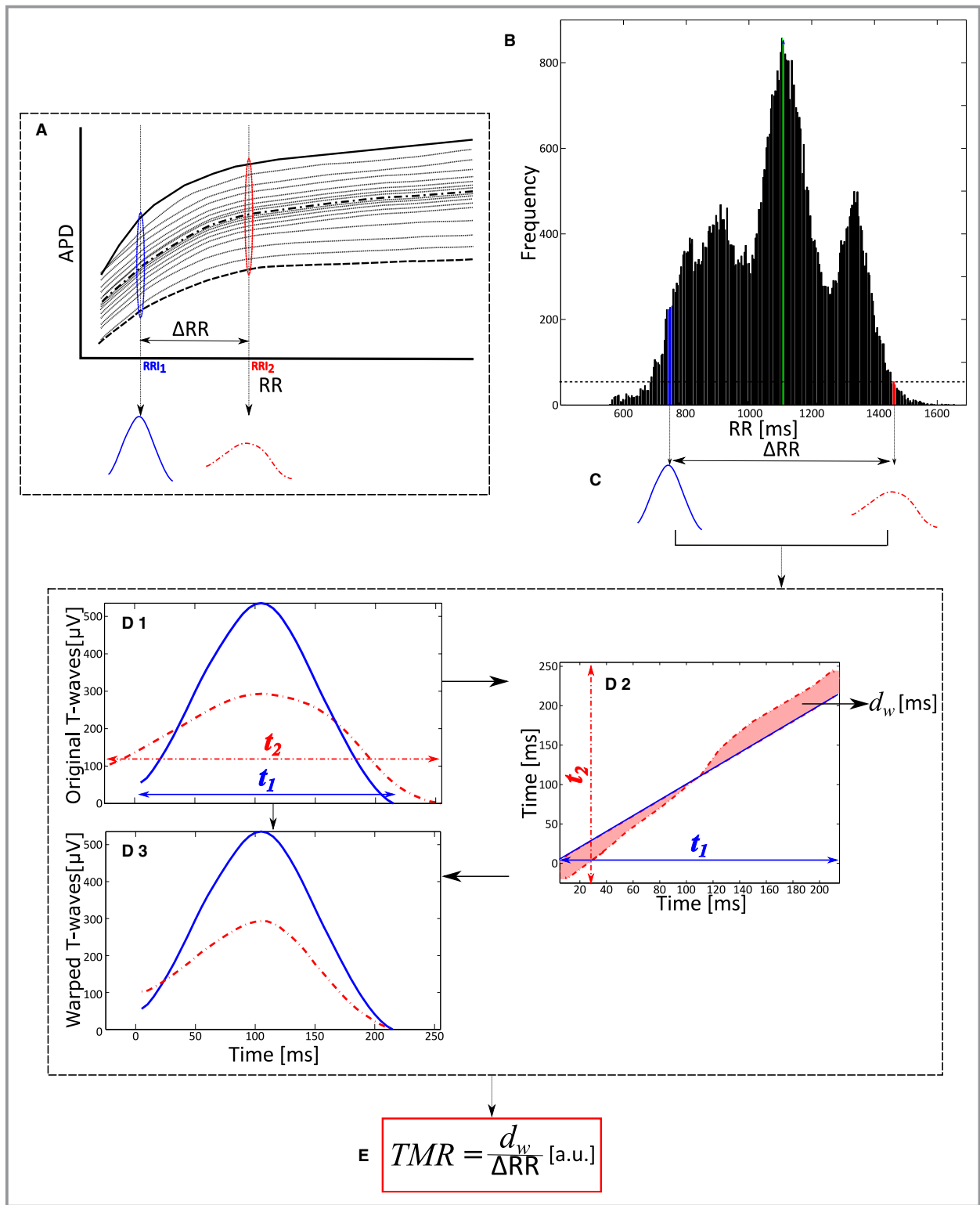
Figure 1. Quantification of the T-wave morphology restitution index. A, Diagram illustrating the hypothesis underlying the proposed methodology: changes in the dispersion of repolarization with RR are reflected as a variation in the morphology of the T-wave with RR. B, RR histogram with bins of RR=10 milliseconds. The green bin shows the median RR interval value. Blue and red bins indicate the RR values defining the maximum intrasubject range. C, Mean warped T-waves of those T-waves associated with the RR values selected in (B). D, Calculation of the index of T-wave morphological difference, d_w, computed by time-warping both mean warped T-waves. E, The index of T-wave morphology restitution, TMR, is calculated as d_w, normalized by the difference between the RR values of both bins, ΔRR. a.u. indicates adimensional units.

corresponding RRIs. For each beat, there is an association between the APD dispersion, representing inhomogeneity in the spatiotemporal organization of the repolarization process, with the T-wave morphology of the surface ECG. Therefore, heterogeneity of restitution properties (illustrated as an increased separation of the restitution curves) corresponds in the ECG with marked differences of T-wave morphology per RR increment. Dispersion of repolarization for a certain RRI (RRI_1) corresponds in the ECG with certain T-wave morphology (Figure 1A, solid blue T-wave). Dispersion of repolarization at a different RRI (RRI_2) corresponds in the ECG with a different T-wave morphology (Figure 1A, dashed red T-wave). Based on previous evidences,[7,8] our hypothesis is that higher variations in the dispersion of repolarization restitution will manifest as higher variations in the T-wave morphology per RR increment, and this will be related to an increased arrhythmic risk. Automatic quantification of the T-wave morphology restitution was performed on every ECG recording in 4 steps:

1. Selection of T-waves. First, the RR histogram was calculated during the entire 24-hour recording, and it was divided into bins 10 milliseconds wide. RR bins with fewer than 50 occurrences were discarded. Next, the 2 most distant RRI bins from the median RRI, distributed symmetrically around this median RRI (Figure 1B, green bin), were chosen as those defining the maximum intrasubject RRI range, ΔRRI (Figure 1B, blue and red bins, respectively), ie, $\Delta RRI = RRI_2 - RRI_1$.
2. Representative T-waves. Two T-waves representative of the average T-wave morphology for RRI_1 and RRI_2 were computed using a warping method recently described by our group.[17] According to our hypothesis, these 2 T-waves, called mean warped T-waves, capture information regarding the dispersion of repolarization at RRI_1 and RRI_2.
3. Quantification of T-wave morphological differences. The morphological differences between the 2 mean warped T-waves were quantified using a previously defined index, d_w.[17] Figure 1.D1 shows both mean warped T-waves, where their morphological difference can be appreciated. Figure 1.D2 shows the nonlinear transformation of the temporal axis of the red-dotted T-wave needed to match the blue-solid T-wave (Figure 1.D3). This transformation is depicted as the red-dotted line in Figure 1D.2. The index d_w quantifies the separation of this line from the diagonal and provides a measure of the T-wave morphological difference along the temporal axis. Note that if this line corresponded to the diagonal, no temporal transformation would be needed, meaning that the morphological differences would be nonexistent ($d_w = 0$).
4. Computation of TMR. TMR is calculated by dividing d_w by ΔRR (Figure 1E) and is a measure of the T-wave morphological change per RR increment.

It is worth noting that the use of mean warped T-waves as representative waves for RRI_1 and RRI_2 minimizes any possible distortion due to short-term memory of repolarization with respect to RRI history.[13] In fact, a representative T-wave obtained by using simple signal averaging might be distorted because the T-waves within a same RRI bin may have different morphologies. This, however, does not occur when using mean warped T-waves as representative waves for each RRI bin because the proposed warping stretches and shrinks each T-wave along the temporal axis to produce the most representative morphology.[17] This is shown in Figure 2, where the T-waves of 3 beats with the same current RRI but different RRI history are presented. The 3 T-waves have slightly different morphologies. These differences can be better appreciated in (Figure 2C.1), where 50 T-waves corresponding to the same RRI but different RRI history are plotted together. A simple signal averaging of these T-waves would have resulted in a distorted mean T-wave, whereas warping ensures that the most representative morphology is computed (Figure 2C.2).

Computation of Other ECG-Based Indices

The markers $\Delta\alpha^{QT}$ and $\Delta\alpha^{Tpe}$ were quantified as the slopes of the regressions of the QT and Tpe intervals, respectively, plotted against the corresponding RRI, after adjustment for QT and Tpe hysteresis effects, respectively.[12,13]

The index of average alternans (IAA), an index reflecting the average T-wave alternans activity during a 24-hour period, was computed by automatic ECG analysis.[21] Turbulence slope (TS), a parameter measuring the turbulence slope of heart rate turbulence, was calculated[22] considering patients having at least 1 ventricular premature beat during the 24-hour ECG recording.

Statistical Analysis

Two-tailed Mann-Whitney and Fisher exact tests were used for univariate comparison of quantitative and categorical data, respectively. The Mann-Whitney test was used to evaluate the association of TMR with the primary and secondary end points. Provided the significance of the association with the primary end point, the statistical analyses described in the following were only performed considering the primary end point. Correlation was evaluated with a Spearman correlation coefficient. Receiver operating characteristic (ROC) curves were used to test the ability to predict the end point and to set cutoff points for risk stratification. The population was divided into 5 balanced groups, and in each group, the criterion of minimal Euclidean distance from each ROC curve to the upper-left corner was applied to select each threshold.
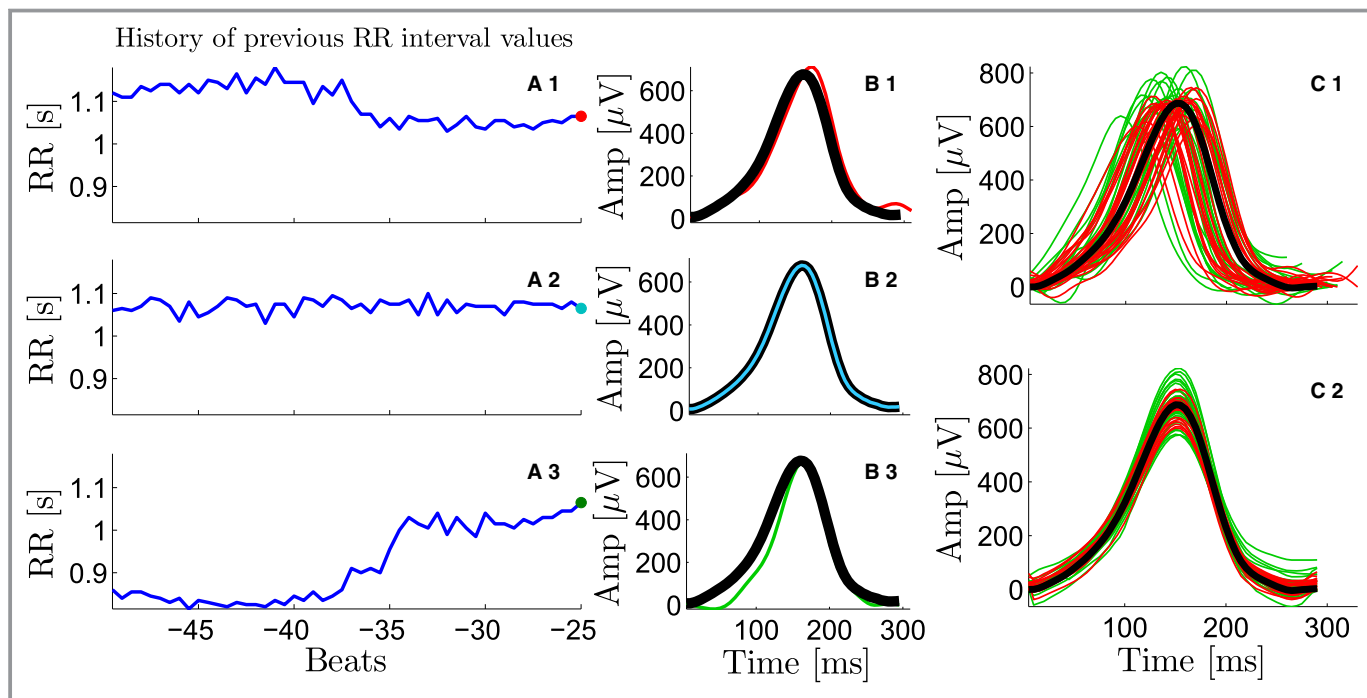
Figure 2. Compensation for the T-wave morphology rate dependence. A1-A3, Three different RR interval (RRI) series previous to a beat with the same RRI. From A1 to A3 the RRI tendency is decreasing, stable, and increasing, respectively. B1-B3, The T-wave for each current beat (in red, cyan, and green, respectively), which depends on the history of previous RRI values. The mean warped T-wave is superimposed and plotted in black. C1-C2, The mean warped T-wave (black), used later for T-wave morphology restitution estimation, compensates for the different histories of RR of each T-wave in the bin. C1, The mean warped T-wave (black) and 50 T-waves from a particular RR bin, where the previous RRI values were longer (red) and shorter (green), respectively, than the current RRI. C2, The mean warped T-wave (black) and the 50 individual T-waves after being warped with respect to the mean warped T-wave.

This was repeated 10 times, and the mean standard deviation of the optimal thresholds was calculated.

To evaluate the robustness of TMR, we computed the Spearman correlation coefficient and the Kendall W coefficient of concordance of TMR calculated during even and odd hours, respectively.

Survival probability was estimated by Kaplan-Meier methods with a comparison of cumulative events performed by using log-rank tests. Patients who died from causes not included in the primary end point were censored at the time of death. Univariate and multivariate Cox regression analyses were performed to determine the predictive value of the risk markers. For multivariate analysis, only the variables with significant association with the primary end point in univariate analysis were included in the model. Two multivariate analyses were performed: multivariate 1, in which the model was adjusted for the clinical and ECG-derived variables and the restitution markers were included 1 at a time; multivariate 2, in which the model was adjusted for the clinical, ECG-derived variables and the restitution markers all at the same time. Backward analysis was applied with a retention criterion of $P<0.05$. A value of $P<0.05$ was considered statistically significant. Statistical analysis was performed using SPSS version 22.0 (SPSS Inc, Chicago, IL).

Results

Clinical Characteristics and Cardiac Events

The study population consisted of 651 consecutive CHF patients with sinus rhythm (464 men, 187 women) aged 18 to 89 years (mean 63 ± 12 years). The majority of patients (82%) were in heart failure NYHA class II, and the remaining 18% were in NYHA class III. LVEF ranged from 10% to 70% with a mean of $37\pm14\%$. The detailed characteristics of the study population are shown in Table 1. No medications were withdrawn during Holter monitoring in any of the patients. During the follow-up there were 148 deaths (23%), including 122 CD (19%) and 26 non-CD (4%). Among the 122 CDs, 55 were SCD and 67 were PFD.

Association of TMR With Clinical Data, ECG-Derived Markers, and Cardiac Events

The 25th, 50th, and 75th percentiles of TMR were 0.030, 0.040, and 0.053, respectively. TMR was significantly higher in SCD and CD victims, as compared with non-SCD and non-CD victims, respectively (Figure 3A). The index $\Delta\alpha^{Tpe}$ was also significantly higher in SCD victims, as compared with the rest of the patients (Figure 3C).[23] The

Table 1. Clinical Characteristics of Patients in the Overall Population and When Classified According to the Index TMR

Variable	Overall Population (n=651)	TMR <0.040 (n=340)	TMR ≥0.040 (n=311)	P Value
Clinical variables				
Age, y	64 (17)	63 (18)	66 (17)	0.155
Sex (male)	464 (71%)	263 (77%)	201 (65%)	<0.001*
NYHA class III	115 (18%)	62 (18%)	53 (17%)	0.758
LVEF ≤35%	356 (55%)	190 (56%)	166 (53%)	0.529
Ischemic etiology	327 (50%)	153 (45%)	174 (56%)	0.006*
Diabetes mellitus	244 (38%)	119 (35%)	125 (40%)	0.195
β-Blockers	455 (70%)	237 (70%)	218 (70%)	0.932
Amiodarone	61 (9%)	27 (8%)	34 (11%)	0.226
ARB or ACE inhibitors	576 (89%)	303 (89%)	273 (88%)	0.624
ECG variables				
Median RR, s	0.86 (0.18)	0.86 (0.17)	0.84 (0.21)	0.027*
RR range, s	0.42 (0.22)	0.45 (0.20)	0.37 (0.21)	<0.001*
QRS >120 ms	262 (40%)	152 (45%)	110 (35%)	0.016*
NSVT and more than 240 VPB in 24-h	168 (26%)	87 (26%)	81 (26%)	0.929
IAA ≥3.7 μV	153 (24%)	74 (22%)	79 (25%)	0.309
TS ≤2.5 ms/RR	281 (47%)	125 (40%)	156 (55%)	<0.001*
T-wave restitution parameters				
$\Delta\alpha^{Tpe}$	0.025 (0.03)	0.020 (0.03)	0.032 (0.04)	<0.001*
$\Delta\alpha^{QT}$	0.199 (0.10)	0.188 (0.08)	0.215 (0.10)	<0.001*

Data are represented as median (interquartile range) for continuous variables and as number (percentage) for dichotomized variables. ACE indicates angiotensin-converting enzyme; ARB, angiotensin receptor blocker; ECG, electrocardiogram; IAA, index of average alternans; LVEF, left ventricular ejection fraction; NSVT, nonsustained ventricular tachycardia; NYHA, New York Heart Association; TMR, T-wave morphology restitution; TS, turbulence slope; VPB, ventricular premature beat.
*Indicates statistical differences.

index $\Delta\alpha^{QT}$ did not show association with any end point (Figure 3B).

The area under the ROC curve was 0.67, 95%CI 0.60 to 0.74, and the optimal threshold for SCD risk stratification was 0.040, with a mean standard deviation of 0.008. Therefore, patients were dichotomized into TMR<0.040 and TMR≥0.040 groups. Of the 651 patients studied, 340 (52%) were included in the TMR<0.040 group, and 311 (48%) in the TMR≥0.040 group. The area under the ROC curve for $\Delta\alpha^{QT}$ was 0.54 (95%CI 0.46 to 0.62, P=0.295). Its optimal cutoff point was set at $\Delta\alpha^{QT}$=0.228. The area under the ROC curve for $\Delta\alpha^{Tpe}$ was 0.63 (95%CI 0.55 to 0.73, P=0.002). Its optimal cutoff point was set at $\Delta\alpha^{Tpe}$=0.028.

Patients in the TMR≥0.040 group, as compared with patients in the TMR<0.040 group, were more frequently females, more frequently had ischemic etiology, showed lower values of median RR, RR range, and QRS width, and higher values of $\Delta\alpha^{QT}$ and $\Delta\alpha^{Tpe}$ (Table 1).

Robustness of TMR

The Spearman correlation coefficient between TMR calculated in the even and the odd hours was 0.7338

(P<0.001), while the Kendall W coefficient of concordance was 0.8669.

Survival Analysis

Univariate Cox analysis revealed that TMR was the variable with the highest hazard ratio (Table 2). No significant association was found between TMR and CD or PFD. The only clinical or ECG-derived indices with significant association with SCD were sex, NYHA class, LVEF, TS, IAA, nonsustained ventricular tachycardia with more than 240 ventricular premature beats in 24 hours, and the range of RR. The duration of the QRS complex was not associated with SCD risk. Regarding the interval-based indices of repolarization restitution, $\Delta\alpha^{QT}$≥0.228 and $\Delta\alpha^{Tpe}$≥0.028 were also associated with SCD (Table 2). Figure 4 shows Kaplan-Meier event probabilities of SCD for the 2 groups defined by TMR (Figure 4A), $\Delta\alpha^{QT}$ (Figure 4B), and $\Delta\alpha^{Tpe}$ (Figure 4C). Table 3 shows the univariate hazard ratios of TMR for SCD risk prediction in the overall population and when it is divided according to different clinical variables.
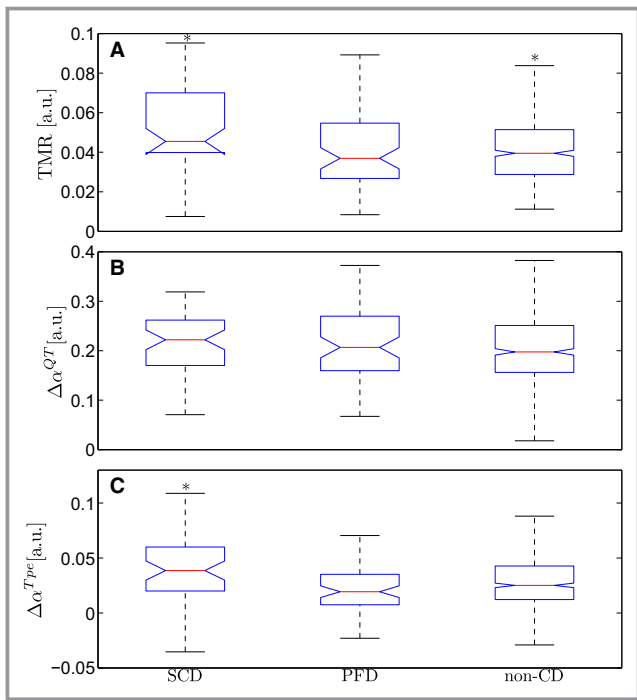
Figure 3. Box plots of T-wave morphology restitution, TMR, (A) and slopes of the regressions of the QT, $\Delta\alpha^{QT}$ (B) and Tpe, $\Delta\alpha^{Tpe}$ (C) intervals for the 3 outcomes: sudden cardiac death (SCD), pump failure death (PFD), and noncardiac death (CD) victims. *Indicates significant differences with respect to the group of patients with the other 2 outcomes.

In multivariate Cox analysis 1, the variables that remained significant were sex, NYHA class, TS, and IAA, with LVEF showing borderline significance. When the restitution markers were added one at a time, TMR was the most significant variable associated with SCD risk and the one with the highest hazard ratio, followed by $\Delta\alpha^{Tpe}$ (Table 2). In multivariate Cox analysis 2, sex, NYHA class, LVEF (borderline), IAA, $\Delta\alpha^{Tpe}$, and TMR were the variables that remained significantly associated with SCD, with the latter being the variable with most significant association and the highest hazard ratio.

Discussion

In this study we proposed a new ECG-derived index, TMR, as a SCD risk predictor in CHF patients. The proposed index quantifies the T-wave morphological change per RR increment and thus represents the restitution of the T-wave morphology. The main result of this study is that TMR specifically predicted SCD, with no association with PFD. TMR was the strongest predictor of SCD, independently of clinical variables such as the LVEF or the NYHA class, other ECG-derived risk indices, such as the T-wave alternans, the QRS duration, or the heart rate turbulence, and other restitution indices such as $\Delta\alpha^{QT}$ and $\Delta\alpha^{Tpe}$.

In a population of CHF patients the most common causes of death are SCD and PFD.[1] The treatment is specific for each group, with implantable cardioverter defibrillators reducing mortality rates of SCD[2] and cardiac resynchronization therapy decreasing PFD rates.[24] Noninvasive markers specific for each mode of CD are of high importance. Several SCD risk markers have been proposed in the literature based on cardiac function (LVEF), arrhythmic features (number and morphology of ventricular premature beats), or autonomic modulation (heart rate turbulence and variability). Most of those markers are also associated with PFD and have a reduced specificity for SCD risk prediction.[22,25,26] In our study, we demonstrate that TMR is a specific marker of SCD with no relation to PFD risk (Figure 3A).

The performance of TMR has been compared with those of 2 other ECG markers characterizing the restitution of the QT and Tpe intervals. Increased values of $\Delta\alpha^{QT}$ have been related to arrhythmic risk in dilated cardiomyopathy[27] and in CHF[28] patients. In our study, $\Delta\alpha^{QT}$ was associated with SCD only when dichotomized. In addition, when it was added to the multivariate model, no association with SCD was found, indicating that it does not contain additional information to that already present in clinical and ECG-derived indices. The index $\Delta\alpha^{Tpe}$ has previously been shown to be related to increased SCD risk.[23] Still, TMR demonstrated a stronger association with SCD risk than $\Delta\alpha^{Tpe}$ in a multivariate analysis. This strengthens the hypothesis that the quantification of the overall T-wave morphological variations is a better estimate of the heterogeneity of repolarization restitution than interval-based markers. Future studies will be needed to assess the relation between TMR and other restitution indices, such as the recently proposed R212 index.[29,30]

Regarding the comparison with clinical and other ECG-derived indices, TMR showed the highest hazard ratio in both univariate and multivariate Cox analyses (Table 2). This suggests that TMR contains specific information on arrhythmia not included in other variables such as LVEF, NYHA class, T-wave alternans, QRS duration, or heart rate turbulence. Lower RRI range was more frequent in patients with higher TMR (Table 1). The range of RRI was marginally associated with SCD in univariate analysis ($P<0.035$), but it did not reach statistical significance in multivariate analysis. Because the RRI range is, in a way, a measure of heart rate variability similar to the triangular interpolation of RR interval histogram index,[31] the following heart rate variability indices were additionally calculated: the standard deviation of RRIs, the standard deviation of the averages of RRIs in 5-minute segments of the entire ECG recording, the root mean-square of successive differences of adjacent RRIs, and the percentage of pairs of adjacent RRIs differing by more than 50 milliseconds. None of these parameters was found to be associated with increased SCD risk in univariate or

al Research

Table 2. Association of the Restitution Markers With SCD

	Univariate		Multivariate 1*		Multivariate 2†	
	HAR (95%CI)	P Value	HAR (95%CI)	P Value	HAR (95%CI)	P Value
Clinical variables						
Male sex	2.14 (1.05–4.38)	0.037‡	2.27 (1.06–4.85)	0.035‡	2.85 (1.32–6.14)	0.008‡
NYHA class III	2.21 (1.23–3.95)	0.008‡	1.95 (1.03–3.68)	0.039‡	2.63 (1.40–4.95)	0.003‡
LVEF ≤35%	2.35 (1.30–4.25)	0.005‡	1.87 (0.98–3.55)	0.057	1.95 (1.03–3.70)	0.041‡
ECG variables						
TS ≤2.5 ms/RR	2.64 (1.45–4.80)	0.001‡	2.26 (1.23–4.17)	0.009‡	1.70 (0.91–3.17)	0.095
IAA ≥3.7 μV	2.33 (1.36–3.99)	0.002‡	2.14 (1.21–3.79)	0.009‡	2.36 (1.33–4.20)	0.003‡
NSVT and >240 VPB/24-h	2.08 (1.22–3.57)	0.008‡	1.25 (0.68–2.29)	0.468	1.37 (0.75–2.50)	0.314
RR range (per 1-SD increment)	0.75 (0.57–0.98)	0.035‡	0.97 (0.71–1.31)	0.826	1.13 (0.83–1.55)	0.429
Restitution markers						
TMR ≥0.040	2.81 (1.57–5.02)	0.001‡	3.27 (1.76–6.11)	<0.001‡	2.94 (1.57–5.53)	0.001‡
$\Delta\alpha^{QT}$ ≥0.228	1.79 (1.06–3.04)	0.031‡	1.47 (0.83–2.63)	0.190	1.16 (0.62–2.15)	0.648
$\Delta\alpha^{Tpe}$ ≥0.028	2.61 (1.47–4.62)	0.001‡	2.92 (1.59–5.33)	0.001‡	2.42 (1.32–4.44)	0.004‡

ECG indicates electrocardiogram; HAR, hazard ratio; IAA, index of average alternans; LVEF, left ventricular ejection fraction; NSVT, nonsustained ventricular tachycardia; NYHA, New York heart Association; TMR, T-wave morphology restitution; TS, turbulence slope; VPB, ventricular premature beat.
*Multivariate 1 includes all clinical and ECG variables at the same time, and the restitution markers are included 1 at a time.
†Multivariate 2 includes all clinical, ECG, and restitution markers at the same time.
‡Indicates significant predictive value.

multivariate Cox analyses, supporting previous studies reporting a limited role of these parameters in predicting SCD among CHF patients.[32,33] Also, the significance of the association between TMR and SCD did not change when any of these parameters was introduced into the multivariate model.

Subpopulation analysis (Table 3) showed that the prognostic value of TMR≥0.040 was mostly due to its association with SCD in patients with depressed LVEF. Importantly, the combination of LVEF≤35% and TMR≥0.040 in a single score resulted in a 60% increase in the hazard ratio, suggesting that TMR captures information related to the electrophysiological substrate that complements systolic function markers and improves prediction. Also, it must be noted that the lack of association of TMR with SCD in some of the subpopulations in Table 3 may be due to their small size.

Indices specifically measuring nonlinear morphological changes[17] were not predictive in this study, suggesting that only linear alterations in the temporal domain of the T-wave are relevant for SCD prediction.

Physiological Interpretation

Based on previous studies reporting that the T-wave morphology reflects the spatio-temporal dispersion of repolarization,[14–16] and that dispersion of repolarization changes with heart rate,[4–6] we hypothesized that the morphology of the

T-wave would vary when measured at different heart rate values. TMR may therefore be in some way related to the spatial heterogeneity of APD restitution. Our results show that TMR is specifically associated with SCD risk, with SCD victims presenting higher TMR values, ie, increased variations in the morphology of the T-wave per RR increment. These results together with our postulated hypothesis help to support the view that increased variations in dispersion of repolarization per RR increment are associated with increased SCD risk, in concordance with previously reported experimental results.[7,8]

Technical Considerations

It is well known that the repolarization response to changes in heart rate is not immediate, and a time lag exists in the adaptation of repolarization.[13] This hysteresis was compensated for the calculation of $\Delta\alpha^{QT}$ and $\Delta\alpha^{Tpe}$.[13] Compensating the memory of the T-wave morphology with the method used for $\Delta\alpha^{QT}$ and $\Delta\alpha^{Tpe}$ [13] is not straightforward. To overcome this difficulty, we calculated an average of at least 50 T-waves recorded at the same RR but at different time instants, ie, different history of RR. Thus, we expected a significant reduction of the hysteresis effect. Still, the calculation of the proposed index TMR was repeated by considering stable heart rate conditions as defined in the following. In each bin the T-wave associated with the RRI history of 50 previous RRIs with the lowest standard deviation was selected (median and

: 10.1161/JAHA.116.005310   Journal of the American Heart Association   8
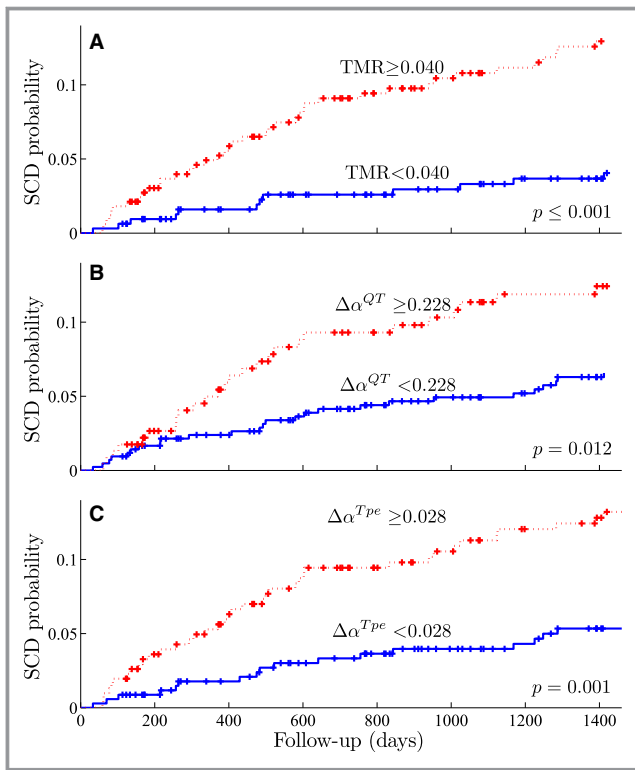
Figure 4. Kaplan-Meier event probability curves of sudden cardiac death (SCD) for the 2 groups defined by T-wave morphology restitution, TMR (A), and slopes of the regressions of the QT, $\Delta\alpha^{QT}$ (B) and Tpe, $\Delta\alpha^{Tpe}$ (C) intervals.

interquartile range of 8 [6] milliseconds and 14 [12] milliseconds for the low and high RRI bins, respectively). Note that the median (interquartile range) value of the mean RRI for the

Table 3. Univariate Association of TMR With SCD in Different Populations

	HAR (95%CI)	P Value
Overall population (n=651)	2.81 (1.57-5.02)	0.001*
Female population (n=187)	2.56 (0.53-12.31)	0.252
Male population (n=464)	3.19 (1.70-5.97)	<0.001*
NYHA class II (n=536)	3.22 (1.57-6.60)	0.001*
NYHA class III (n=115)	2.32 (0.84-6.39)	0.104
LVEF ≤35% (n=356)	3.27 (1.64-6.56)	0.001*
LVEF >35% (n=295)	2.10 (0.72-6.15)	0.175
Amiodarone (n=61)	1.73 (0.32-9.44)	0.528
No amiodarone (n=590)	2.97 (1.60-5.52)	0.001*
Ischemic (n=327)	2.52 (1.17-5.43)	0.018*
Nonischemic (n=324)	2.97 (1.21-7.29)	0.017*

HAR indicates hazard ratio; LVEF, left ventricular ejection fraction; NYHA, New York Heart Association Class; SCD, sudden cardiac death; TMR, T-wave morphology restitution.
*Indicates significant predictive value.

low and high RRI was 645 (155) milliseconds and 1035 (253) milliseconds, respectively. The Spearman correlation coefficient between these new values of TMR and those obtained with our proposed methodology was calculated, obtaining a value of 0.60, $P<10^{-64}$. A Mann-Whitney test showed that the median TMR value calculated for stable heart rate conditions was also significantly higher in SCD victims as compared with the rest of the patients, but to a lesser extent than the original TMR values ($P=0.039$ versus $P<10^{-3}$). A possible explanation for this difference can be that, although T-waves with the most stable RR history are considered, steady state is difficult to find in Holter ECG recordings. A mean warped T-wave of different T-waves coming from RR values with different histories may thus be a better solution, as illustrated in Figure 2.

The computation of TMR does not require a minimum recording duration. However, a wide RR range is recommended to ensure an appreciable variation in the morphology of the T-wave. In addition, the methodology requires sinus rhythm. TMR was computable in all patients available for the study, and there were no artifacts or unusable portions of the Holter ECGs limiting its measurement. Also, in contrast with beat-to-beat repolarization metrics, TMR is not affected by ventricular premature beats, and it only requires waveforms from few beats at different RRIs to be computed.

Regarding the robustness of TMR, we showed that there was a strong correlation and concordance between the TMR indices computed at even and odd hours, indicating that the index presents an adequate repeatability and stability.

Because SCD and PFD are both common end points in the study population, PFD might be a competing risk for SCD. The cumulative incidence function of SCD using data from the competing risk was estimated,[34] and a Gray test was applied to evaluate the equality of the cumulative incidence functions across groups.[35] The cumulative incidence functions were found to be very similar to the Kaplan-Meier curves, and Gray test P-value was almost equal to log-rank test P-value ($P=0.00017$ versus $P=0.00028$). Thus, ignoring the informative censoring mechanism (PFD) did not substantially influence the estimates of SCD.

Limitations

Prospective studies are needed to verify that the observations presented here have a role in SCD prediction in CHF patients. This study only considered consecutive patients, so the number of SCD victims was low, and this has limited the possibility of performing further statistical analyses. Because this is a retrospective study, further investigations on the applicability of the defined cutoff point and on the extension of the analysis to other CHF and non-CHF populations are needed to confirm the prognostic value of the proposed index.

Also, the T-wave morphology is related to the lead configuration; however, spatial dependency of TMR is small because TMR measures changes within a mathematically constructed lead that represents global repolarization.

Conclusion

This study demonstrates that an ECG-derived index, TMR, quantifying the T-wave morphology restitution, is strongly associated with SCD in a population of CHF patients. TMR showed higher predictive value than other clinical variables such as LVEF or NYHA class and other ECG-derived indices such as the T-wave alternans, the QRS duration, or the heart rate turbulence.

Acknowledgments

J.R. would like to acknowledge Alba Martín for her valued help during the peer-review process.

Sources of Funding

Disclosures

None.

References

1. Darbar D. Genomics, heart failure and sudden cardiac death. *Heart Fail Rev*. 2010;15:229–238.

2. Mark DB, Nelson CL, Anstrom KJ, Al-Khatib SM, Tsiatis AA, Cowper PA, Clapp-Channing NE, Davidson-Ray L, Poole JE, Johnson G, Anderson J, Lee KL, Bardy GH. Cost-effectiveness of defibrillator therapy or amiodarone in chronic stable heart failure results from the sudden cardiac death in heart failure trial (SCD-HeFT). *Circulation*. 2006;114:135–142.

3. Laurita KR, Girouard SD, Rosenbaum DS. Modulation of ventricular repolarization by a premature stimulus role of epicardial dispersion of repolarization kinetics demonstrated by optical mapping of the intact guinea pig heart. *Circ Res*. 1996;79:493–503.

4. Glukhov AV, Fedorov VV, Lou Q, Ravikumar VK, Kalish PW, Schuessler RB, Moazami N, Efimov IR. Transmural dispersion of repolarization in failing and nonfailing human ventricle. *Circ Res*. 2010;106:981–991.

5. Srinivasan NT, Orini M, Simon RB, Providência R, Khan FZ, Segal OR, Babu GG, Bradley R, Rowland E, Ahsan S, Chow AW, Lowe MD, Taggart P, Lambiase PD. Ventricular stimulus site influences dynamic dispersion of repolarization in the intact human heart. *Am J Physiol Heart Circ Physiol*. 2016;311:H545–H554.

6. Orini M, Taggart P, Srinivasan N, Hayward M, Lambiase PD. Interactions between activation and repolarization restitution properties in the intact human heart: in-vivo whole-heart data and mathematical description. *PLoS One*. 2016;11:e0161765.

7. Pak H, Hong SJ, Hwang GS, Lee HS, Park S, Ahn JC, Ro YM, Kim Y. Spatial dispersion of action potential duration restitution kinetics is associated with induction of ventricular tachycardia/fibrillation in humans. *J Cardiovasc Electrophysiol*. 2004;15:1357–1363.

8. Nash MP, Bradley CP, Sutton PM, Clayton RH, Kallis P, Hayward MP, Paterson DJ, Taggart P. Whole heart action potential duration restitution properties in cardiac patients: a combined clinical and modelling study. *Exp Physiol*. 2006;91:339–354.

9. Yue AM, Franz MR, Roberts PR, Morgan JM. Global endocardial electrical restitution in human right and left ventricles determined by noncontact mapping. *J Am Coll Cardiol*. 2005;46:1067–1075.

10. Zabel M, Acar B, Klingenheben T, Franz MR, Hohnloser SH, Malik M. Analysis of 12-lead T-wave morphology for risk stratification after myocardial infarction. *Circulation*. 2000;102:1252–1257.

11. Mincholé A, Pueyo E, Rodríguez JF, Zacur E, Doblaré M, Laguna P. Quantification of restitution dispersion from the dynamic changes of the T-wave peak to end, measured at the surface ECG. *IEEE Trans Biomed Eng*. 2011;58:1172–1182.

12. Zareba W, De Luna AB. QT dynamics and variability. *Ann Noninvasive Electrocardiol*. 2005;10:256–262.

13. Pueyo E, Smetana P, Caminal P, De Luna AB, Malik M, Laguna P. Characterization of QT interval adaptation to RR interval changes and its use as a risk-stratifier of arrhythmic mortality in amiodarone-treated survivors of acute myocardial infarction. *IEEE Trans Biomed Eng*. 2004;51:1511–1520.

14. Van Oosterom A. Genesis of the T-wave as based on an equivalent surface source model. *J Electrocardiol*. 2001;34:217–227.

15. Xue J, Chen Y, Han X, Gao W. Electrocardiographic morphology changes with different type of repolarization dispersions. *J Electrocardiol*. 2010;43:553–559.

16. Meijborg VMF, Conrath CE, Opthof T, Belterman CNW, de Bakker JMT, Coronel R. Electrocardiographic T-wave and its relation with ventricular repolarization along major anatomical axes. *Circ Arrhythm Electrophysiol*. 2014;7:524–531.

17. Ramírez J, Orini M, Tucker JD, Pueyo E, Laguna P. Variability of ventricular repolarization dispersion quantified by time-warping the morphology of the T-waves. *IEEE Trans Biomed Eng*. 2016. Available at: http://ieeexplore.ieee.org/document/7582410/?reload=true. Accessed May 13, 2017.

18. Vázquez R, Bayés-Genís A, Cygankiewicz I, Pascual-Figal D, Grigorian-Shamagian L, Pavon R, Gonzalez-Juanatey JR, Cubero JM, Pastor L, Ordonez-Llanos J, Cinca J, De Luna AB. The MUSIC Risk score: a simple method for predicting mortality in ambulatory patients with chronic heart failure. *Eur Heart J*. 2009;30:1088–1096.

19. Castells F, Laguna P, Sörnmo L, Bollmann A, Millet J. Principal component analysis in ECG signal processing. *EURASIP J Appl Signal Processing*. 2007;2007:98–98.

20. Martínez JP, Almeida R, Olmos S, Rocha AP, Laguna P. A wavelet-based ECG delineator: evaluation on standard databases. *IEEE Trans Biomed Eng*. 2004;51:570–581.

21. Monasterio V, Laguna P, Cygankiewicz I, Vázquez R, Bayés-Genís A, De Luna AB, Martínez JP. Average T-wave alternans activity in ambulatory ECG records predicts sudden cardiac death in patients with chronic heart failure. *Heart Rhythm*. 2012;9:383–389.

22. Cygankiewicz I, Zareba W, Vázquez R, Vallverdu M, Gonzalez-Juanatey JR, Valdes M, Almendral J, Cinca J, Caminal P, De Luna AB. Heart rate turbulence predicts all-cause mortality and sudden death in congestive heart failure patients. *Heart Rhythm*. 2008;5:1095–1102.

23. Ramírez J, Monasterio V, Mincholé A, Llamedo M, Lenis G, Cygankiewicz I, De Luna AB, Malik M, Martínez JP, Laguna P, Pueyo E. Automatic SVM classification of sudden cardiac death and pump failure death from autonomic and repolarization ECG markers. *J Electrocardiol*. 2015;48:551–557.

24. Neragi-Miandoab S. Non-transplant surgical therapy options of heart failure. *Minerva Cardioangiol*. 2014;62:481–496.

25. Buxton AE, Lee KL, Hafley GE, Pires LA, Fisher JD, Gold MR, Josephson ME, Lehmann MH, Prystowsky EN. Limitations of ejection fraction for prediction of sudden death risk in patients with coronary artery disease: lessons from the MUSTT study. *J Am Coll Cardiol*. 2007;50:1150–1157.

26. Moss AJ, Davis HT, DeCamilla J, Bayer LW. Ventricular ectopic beats and their relation to sudden and nonsudden cardiac death after myocardial infarction. *Circulation*. 1979;60:998–1003.

27. Szydlo K, Trusz-Gluza M, Wita K, Filipecki A, Orszulak W, Urbanczyk D, Krauze J, Kolasa J, Tabor Z. QT/RR relationship in patients after remote anterior myocardial infarction with left ventricular dysfunction and different types of ventricular arrhythmias. *Ann Noninvasive Electrocardiol*. 2008;13:61–66.

28. Iacoviello M, Forleo C, Guida P, Romito R, Sorgente A, Sorrentino S, Catucci S, Mastropasqua F, Pitzalis M. Ventricular repolarization dynamicity provides independent prognostic information toward major arrhythmic events in patients with idiopathic dilated cardiomyopathy. *J Am Coll Cardiol*. 2007;50:225–231.

29. Nicolson WB, McCann GP, Brown PD, Sandilands AJ, Stafford PJ, Schlindwein FS, Samani NJ, Ng GA. A novel surface electrocardiogram-based marker of ventricular arrhythmia risk in patients with ischemic cardiomyopathy. *J Am Heart Assoc*. 2012;1:e001552. https://doi.org/10.1161/jaha.112.001552.

30. Nicolson WB, McCann GP, Smith MI, Sandilands AJ, Stafford PJ, Schlindwein FS, Samani NJ, Ng GA. Prospective evaluation of two novel ECG-based restitution biomarkers for prediction of sudden cardiac death risk in ischaemic cardiomyopathy. *Heart*. 2014;100:1878–1885.

31. Task Force of the European Society of Cardiology and the North American Society of Pacing and Electrophysiology . Heart rate variability. Standards of measurement, physiological interpretation, and clinical use. *Eur Heart J*. 1996;17:354–381.

32. La Rovere MT, Pinna GD, Maestri R, Mortara A, Capomolla S, Febo O, Ferrari R, Franchini M, Gnemmi M, Opasich C, Riccardi PG, Traversi E, Cobelli F. Short-term heart rate variability strongly predicts sudden cardiac death in chronic heart failure patients. *Circulation*. 2003;107:565–570.

33. Wu L, Jiang Z, Li C, Shu M. Prediction of heart rate variability on cardiac sudden death in heart failure patients: a systematic review. *Int J Cardiol*. 2014;174:857–860.

34. Scrucca L, Santucci A, Aversa F. Competing risk analysis using R: an easy guide for clinicians. *Bone Marrow Transplant*. 2007;40:381–387.

35. Gray RJ. A class of K-sample tests for comparing the cumulative incidence of a competing risk. *Ann Stat*. 1988;16:1141–1154.